Sliding Mode Control for High-Precision Motion of a Piezostage

Khalid Abidi and Asif Šabanovic, *Senior Member, IEEE*

***Abstract*—In this paper, control of piezostage using sliding mode control (SMC) method is presented. Due to the fast dynamics of the piezostage and since high accuracy is required the special attention is paid to avoid chattering. The presence of hysteresis characteristics represents main nonlinearity in the system. Structure of proposed SMC controller is proven to offer chattering-free motion and rejection of the disturbances represented by hysteresis and the time variation of the piezostack parameters. In order to enhance the accuracy of the closed loop system, a combination of disturbance rejection method and the SMC controller is explored and its effectiveness is experimentally demonstrated. The disturbance observer is constructed using a second-order lumped parameter model of the piezostage and is based on SMC framework. Closed-loop experiments are presented using proportional-integral-derivative controller and sliding mode controller with disturbance compensation for the purpose of comparison.**

***Index Terms*—Discrete-time control, high-precision motion, piezostage, sliding mode control (SMC).**

I. Introduction

PIEZOELECTRIC actuators have shown a great potential in applications that require submicrometer down to nanometer motion. The advantages that piezoelectric actuators offer are the absence of friction and stiction characteristics that exist in other actuators. Thus, piezoelectric actuators are ideal for very high-precision-motion applications. The main characteristics of piezoelectric actuators are: extremely high resolution in the nanometer range, high bandwidth up to several kilohertz range, a large force up to few tons, and very short travel in the submillimeter range (see [1]). Application areas of piezoelectric actuators include: micromanipulation, microassembly, add-ons for high-precision cutting machinery, and as secondary actuators in macro/micromotion systems such as dual-stage hard-disk drives. In all of these applications, the accuracy of positioning is very important and in many cases the closed loop control is the only answer. Despite this, there are many attempts (see [2] and [3]) to drive piezoelectric actuators as an open loop system with fine compensation of the hysteresis nonlinearity in one or another way. With development of accurate position transducers, the possibility to use robust feedback-based nonlinear control methods is becoming an attractive alternative to the model-based compensation.

Despite the fact that a piezoelectric actuator is a distributed parameters system, modeling for control purposes is based on a lumped parameters system. It is possible to drive piezoelectric actuators with either voltage or charge as input. The former is easier to implement in hardware and is the most common mode of controlling these actuators. However, a piezoelectric actuator driven by voltage as input will exhibit nonlinearity between the input (voltage) and output (position). This nonlinearity is mainly due to the parasitic hysteresis characteristics of piezoelectric crystals. It has been shown in many other works (see [2]) that hysteresis behavior does not exist in the case of a piezoelectric actuator driven by charge and that the actuator exhibits almost linear behavior between charge and position. However, as mentioned before, hardware realization of charge controllers is very difficult and voltage supply-based control is mostly preferred.

A major difficulty in using piezoelectric actuators is the hysteresis effect, which causes large positioning errors. There are many techniques used in order to handle the nonlinearities brought by this effect such as feedback and model-based feedforward control. Also, in [4], iterative method is used in order to find the hysteresis that compensates feedforward input for high-precision positioning. In addition to the hysteresis characteristics, piezoelectric actuators also have dynamic creep effect that has to be taken into account. In [5], both the hysteresis and dynamic creep effects are given importance and operator-based inverse feedforward controller is applied. It has been shown that this controller works well for highly dynamic operation and that it is simple and inexpensive for mechatronic devices with hysteresis characteristics. There has been also research on the mathematical modeling of hysteresis, such as in [2], [3], [6]–[8] where new results for the modeling of physical hysteresis and its applications in dynamic research are shown. Complicated models of the hysteresis allow for accurate control of these actuators but are limited due to presence of other internal disturbances such as creep. In [2], complex and accurate model of hysteresis is presented, but is hard to implement and too complex for control applications. In [3], [6], and [7], simpler models of hysteresis are proposed, however, those models fail to precisely represent hysteresis behavior throughout the whole range of input voltage of the piezoelectric actuator. The problem of hysteresis was also approached by using neural-network (NN) technology. In [9], they trained a recurrent NN to mimic the behavior of inverse characteristic of the piezocrystal and they used this trained network in series with the piezoactuator.

Manuscript received November 11, 2004; revised August 1, 2006. Abstract published on the Internet September 15, 2006.

K. Abidi is with the Department of Electrical and Computer Engineering, National University of Singapore, Singapore 117576, Singapore (e-mail: kabidi@nus.edu.sg).

A. Šabanovic is with the Department of Electrical Engineering and Computer Science, Sabanci University, Istanbul, Turkey (e-mail: asif@sabanciuniv.edu.tr).

Digital Object Identifier 10.1109/TIE.2006.885477

Use of a hysteresis model provides some advantages; it does not need the measurement of the mechanical coordinates and is helpful in applications where the use of sensors for position measurement is impractical.

In [7], $H\infty$-based closed-loop control is presented with model-based hysteresis compensation. While the method produces good results, it can be made simpler if the hysteresis model-based compensation is replaced with a simpler methodology. In [10], a NN-based feed-forward assisted proportional-integral-derivative (PID) controller was proposed. A hybrid control strategy using a variable structure control is suggested for submicrometer positioning control [9], [11]. These methods need an explicit system model for the control design, and the performance achievable depends on the accuracy of the model. In [14], a sliding-mode approach for linear discrete-time systems is proposed. Based on the proposed method in [14] and [17], $O(T_s^2)$ bound of the sliding surface is achieved. In this paper, we claim the same accuracy, but, with partial knowledge of system dynamics.

In this paper, the aim is to design a motion controller for piezostage having position sensor based on the assumption that the piezostage can be modeled as a linear lumped parameters $(T, m_{\mathrm{eff}}, c_{\mathrm{eff}}, k_{\mathrm{eff}})$ second-order electromechanical system with voltage as the input and position as the output coordinate and hysteresis nonlinearity being the major disturbance effecting the system. Furthermore, it is assumed that the parameters of the model are bounded and have some so-called nominal values $(T_{\mathrm{N}}, m_{\mathrm{N}}, c_{\mathrm{N}}, k_{\mathrm{N}})$.

In this paper, the sliding mode methods are applied in the design of a high-accuracy piezoactuator position. The solution proposed here combines the sliding mode controller and the disturbance rejection method in order to achieve high accuracy in the actuator trajectory tracking. For the disturbance estimation, a sliding mode observer-based disturbance compensation method is used here. By manipulating model of a piezoactuator in a form where nonlinearities due to hysteresis are presented as an additive disturbance acting together with external force to the mechanical system a simple second-order observer is designed to estimate lumped disturbance.

This paper is organized as follows. In Section II, a suitable model of a piezoactuator, based on already known results, is presented. In Section III, the sliding mode-based controller and in Section IV the observer design is presented. In Section V, experimental results verifying theoretical works are presented.

II. Model of the Piezostage

In this paper, a piezostage that consists of a piezodrive integrated with a sophisticated flexure structure for motion amplification is used. The flexure structure is wire-EDM-cut and is designed to have zero stiction and friction. Fig. 1 shows the piezodrive integrated flexure structure.

In addition to the absence of internal friction, flexure stages exhibit high stiffness and high load capacity. Flexure stages are also insensitive to shock and vibration. However, since the piezodrive exhibits nonlinear hysteresis behavior, the overall system will also exhibit the same behavior.

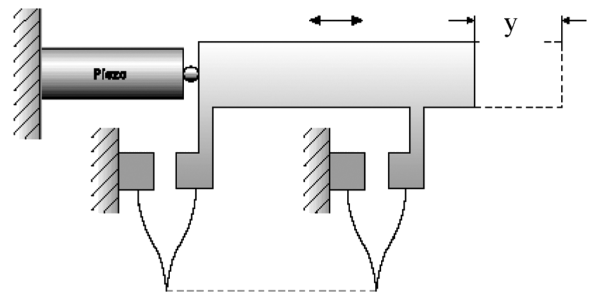

Fig. 1. Structure of a flexure piezostage.

The dynamics of the piezostage can be represented by the following second-order differential equation coupled with hysteresis in the presence of external forces

$$m_{\mathrm{eff}}\ddot{y} + c_{\mathrm{eff}}\dot{y} + k_{\mathrm{eff}}y = T\left(u(t) - h(y,u)\right) - F_{\mathrm{ext}} \quad (1)$$

where m_{eff} denotes the effective mass of the stage, y denotes the displacement of the stage, c_{eff} denotes the effective damping of the stage, k_{eff} denotes the effective stiffness of the stage, T denotes the electromechanical transformation ratio, u denotes the input voltage and $h(y,u)$ denotes the nonlinear hysteresis that has been found to be a function of y and u, [2], and F_{ext} is the external force acting on the stage.

The model represented by (1) is found from the work of [2] and it shows that from the mechanical motion the hysteresis may be perceived as a disturbance force that satisfies matching conditions. This means that the sliding mode-based control should be able to reject the influence of the hysteresis nonlinearity on the mechanical motion. At the same time, it is obvious that the lumped disturbance consisting of the external force acting on the system and the hysteresis can be estimated, thus allowing the application of the disturbance rejection method in the overall system design.

III. Sliding-Mode-Controller Design

A. Controller Design

To facilitate the derivation of the control law, (1) is written into the state-space form

$$\dot{x}_1 = \dot{y} = x_2 \quad (2)$$

$$\dot{x}_2 = \ddot{y} = -\frac{k_{\mathrm{eff}}}{m_{\mathrm{eff}}}x_1 - \frac{c_{\mathrm{eff}}}{m_{\mathrm{eff}}}x_2 + \frac{T}{m_{\mathrm{eff}}}u - \frac{T}{m_{\mathrm{eff}}}h - \frac{F_{\mathrm{ext}}}{m_{\mathrm{eff}}}. \quad (3)$$

It is possible to write (3) in a more general form as shown below

$$\dot{x} = f(x, h, F_{\mathrm{ext}}) + Bu. \quad (4)$$

The aim is to drive the states of the system into the set S defined by

$$S = \{x : G(x^r - x) = \sigma(x, x^r) = 0\} \quad (5)$$

where $G = [\lambda\ 1]$ with λ being a positive constant, x is the state vector $x^{\mathrm{T}} = [x_1\ x_2]$, x_r is the reference vector $(x^r)^{\mathrm{T}} = [x_1^r\ x_2^r]$, and $\sigma(x, x^r)$ is the function defining sliding mode manifold.

The derivation of the control law starts with the selection of the Lyapunov function, $V(\sigma)$, and an appropriate form of the derivative of the Lyapunov function, $\dot{V}(\sigma)$.

For single-input–single-output systems such as (3), required to have motion in manifold (5), natural selection of Lyapunov function candidate seems in the form

$$V(\sigma) = \frac{\sigma^2}{2} \tag{6}$$

Hence, the derivative of the Lyapunov function is

$$\dot{V}(\sigma) = \sigma\dot{\sigma}. \tag{7}$$

In order to guarantee the asymptotic stability of the solution $\sigma(x, x^r) = 0$, the derivative of the Lyapunov function may be selected to be

$$\dot{V}(\sigma) = -D\sigma^2 \tag{8}$$

where D is a positive constant. Hence, if the control can be determined from (7) and (8), the asymptotic stability of solution (5) will be guaranteed since $V(\sigma) > 0$, $V(0) = 0$, and $\dot{V}(\sigma) < 0$, $\dot{V}(0) = 0$. By combining (7) and (8), the following result is obtained

$$\sigma(\dot{\sigma} + D\sigma) = 0. \tag{9}$$

A solution for (9) is as follows

$$\dot{\sigma} + D\sigma = 0. \tag{10}$$

The derivative of the sliding function is as follows

$$\dot{\sigma} = G(\dot{x}^r - \dot{x}) = G\dot{x}^r - G\dot{x}. \tag{11}$$

From (11) and using (4)

$$\dot{\sigma} = \underbrace{G\dot{x}^r - Gf}_{GBu_{\text{eq}}} - GBu(t) = GB\left(u_{\text{eq}} - u(t)\right). \tag{12}$$

If (12) is substituted in (10) and the result is solved for the control

$$u(t) = u_{\text{eq}} + (GB)^{-1}D\sigma. \tag{13}$$

It can be seen from (12) that u_{eq} is difficult to calculate. Using the fact that u_{eq} is a continuous function, (12) can be written in discrete-time form after applying Euler's approximation

$$\frac{\sigma\left((k+1)T_{\text{s}}\right) - \sigma(kT_{\text{s}})}{T_{\text{s}}} = GB\left(u_{\text{eq}}(kT_{\text{s}}) - u(kT_{\text{s}})\right) \tag{14}$$

where T_{s} is the sampling time and $k = Z^+$. It is also necessary to write (13) in discrete-time form just as it was done before

$$u(kT_{\text{s}}) = u_{\text{eq}}(kT_{\text{s}}) + (GB)^{-1}D\sigma(kT_{\text{s}}). \tag{15}$$

If (14) is solved for the equivalent control, the following is obtained

$$u_{\text{eq}}(kT_{\text{s}}) = u(kT_{\text{s}}) + (GB)^{-1}\left(\frac{\sigma\left((k+1)T_{\text{s}}\right) - \sigma(kT_{\text{s}})}{T_{\text{s}}}\right). \tag{16}$$

Since the system is causal, and it is required to avoid calculation of the predicted value for σ, control cannot be dependent on a future value of σ. Having equivalent control as a continuous function, the current value of the equivalent control will be approximated by a single time-step backward value computed from (16) as follows

$$\hat{u}_{\text{eq}_k} \cong u_{\text{eq}_{k-1}} = u_{k-1} + (GB)^{-1}\left(\frac{\sigma_k - \sigma_{k-1}}{T_{\text{s}}}\right) \tag{17}$$

where $\hat{u}_{\text{eq}_k}$ (or $\hat{u}_{\text{eq}}(kT_{\text{s}})$) is the estimate of the current value of the equivalent control. If (17) is substituted in (15)

$$u_k = u_{k-1} + (GBT_{\text{s}})^{-1}\left((DT_{\text{s}} + 1)\sigma_k - \sigma_{k-1}\right). \tag{18}$$

Note that in certain applications where only partial state measurements exist, observers can be used to estimate the unknown states in order to compute σ_k. In this paper, the unknown state is the velocity and is estimated using a discrete derivative. Hence, control (18) is suitable for implementation since it requires measurement of the sliding mode function and value of the control applied in the preceding step. Since, the above control law is derived from discrete-time approximations based on the continuous-time equations. Hence, these approximations will introduce errors in the control that must be analyzed carefully.

B. *Closed-Loop Behavior With the Approximated Control*

As a consequence of the approximations that were made in the derivation of the discrete-time control law, some deviations in the sliding surface from the desired sliding manifold may exist. This deviation of the sliding surface from the desired manifold at each sampling instant will be analyzed. Intersampling behavior is also analyzed.

Considering (4), the derivative of the sliding surface is given by

$$\dot{\sigma}(t) = G(\dot{x}^r - \dot{x}) = G\dot{x}^r - Gf - GBu(t). \tag{19}$$

The discrete-time equivalent of the sliding manifold can be obtained by taking the integral on both sides of (19) from kT_{s} to $(k+1)T_{\text{s}}$

$$\sigma_{k+1} - \sigma_k = \int_{kT_{\text{s}}}^{(k+1)T_{\text{s}}} \left(G\dot{x}^r - Gf - GBu(t)\right)dt. \tag{20}$$

Applying a sample and hold to the control input between consecutive samples $u(t) = u_k$ for $kT_{\text{s}} \le t < (k+1)T_{\text{s}}$

$$\sigma_{k+1} - \sigma_k = \int_{kT_{\text{s}}}^{(k+1)T_{\text{s}}} (G\dot{x}^r - Gf)dt - T_{\text{s}}GBu_k. \tag{21}$$

Using the assumptions that $\dot{x}^r$ and f are smooth and bounded, the integrations in (21) can be approximated by using Euler's integration

$$\sigma_{k+1} = \sigma_k + T_\mathrm{s} G\left(\dot{x}_k^r - f_k\right) - T_\mathrm{s} G B u_k + O\left(T_\mathrm{s}^2\right). \quad (22)$$

Here, $O(T_\mathrm{s}^2)$ is the error introduced due to Euler's integration, [16]. If the control defined by (18) is introduced into (22)

$$\sigma_{k+1} = \sigma_k + T_\mathrm{s} G\left(\dot{x}_k^r - f_k\right) - T_\mathrm{s} G B u_{k-1} - T_\mathrm{s} D\sigma_k - \sigma_k + \sigma_{k-1} + O\left(T_\mathrm{s}^2\right). \quad (23)$$

After some simplifications (23) is reduced to

$$\sigma_{k+1} = T_\mathrm{s} G\left(\dot{x}_k^r - f_k\right) - T_\mathrm{s} G B u_{k-1} - T_\mathrm{s} D\sigma_k + \sigma_{k-1} + O(T_\mathrm{s}^2). \quad (24)$$

AQ1 If $T_\mathrm{s} G(\dot{x}_{k-1}^r - f_{k-1})$ is added and subtracted from the r.h.s of (24), the following is obtained

$$\begin{aligned}\sigma_{k+1} = {} & T_\mathrm{s} G\left(\dot{x}_k^r - f_k\right) - T_\mathrm{s} G\left(\dot{x}_{k-1}^r - f_{k-1}\right) - T_\mathrm{s} D\sigma_k \\ & + \underbrace{T_\mathrm{s} G\left(\dot{x}_{k-1}^r - f_{k-1}\right) - T_\mathrm{s} G B u_{k-1}}_{\sigma_k - \sigma_{k-1} + O(T_\mathrm{s}^2)} \\ & + \sigma_{k-1} + O\left(T_\mathrm{s}^2\right). \end{aligned} \quad (25)$$

After some simplifications, (25) becomes

$$\sigma_{k+1} = \sigma_k - T_\mathrm{s} D\sigma_k + T_\mathrm{s} G\left(\Delta\dot{x}_k^r - \Delta f_k\right) + O\left(T_\mathrm{s}^2\right) \quad (26)$$

where $\Delta\dot{x}_k^r = \dot{x}_k^r - \dot{x}_{k-1}^r$ and $\Delta f_k = f_k - f_{k-1}$. Note that if $D = 1/T_\mathrm{s}$, then the r.h.s of (26) is of order $O(T_\mathrm{s}^2)$, keeping in mind that $\dot{x}^r$ and f are smooth and bounded. Hence

$$\sigma_{k+1} = O\left(T_\mathrm{s}^2\right). \quad (27)$$

Hence, it is shown that the maximum deviation from the sliding surface at each sampling instant is of order $O(T_\mathrm{s}^2)$.

Next, it will be shown that the intersampling deviation of the sliding surface from the desired manifold is also of order $O(T_\mathrm{s}^2)$.

Consider the intersampling instant of $t = kT_\mathrm{s} + \tau$ where $0 \leq \tau \leq T_\mathrm{s}$. If (19) is integrated on both sides from kT_s to $kT_\mathrm{s} + \tau$

$$\sigma(kT_\mathrm{s} + \tau) - \sigma_k = \int\limits_{kT_\mathrm{s}}^{kT_\mathrm{s}+\tau} \left(G\dot{x}^r - Gf - GBu(t)\right) dt. \quad (28)$$

Applying the sample and hold to the control and Euler's integration to the remaining integral gives

$$\sigma(kT_\mathrm{s} + \tau) = \sigma_k + \tau G\left(\dot{x}_k^r - f_k\right) - \tau G B u_k + O(\tau^2). \quad (29)$$

If the control defined by (18) is introduced into (29)

$$\sigma(kT_\mathrm{s} + \tau) = \sigma_k + \tau G\left(\dot{x}_k^r - f_k\right) - \tau G B u_{k-1} - \tau D\sigma_k - \frac{\tau}{T_\mathrm{s}}(\sigma_k - \sigma_{k-1}) + O(\tau^2). \quad (30)$$

If $\tau G(\dot{x}_{k-1}^r - f_{k-1})$ is added and subtracted from the r.h.s of (24) and $D = 1/T_\mathrm{s}$, the following is obtained

$$\begin{aligned}\sigma(kT_\mathrm{s} + \tau) = {} & \sigma_k + \frac{\tau}{T_\mathrm{s}} G\left(T_\mathrm{s}\left(\Delta\dot{x}_k^r - \Delta f_k\right)\right) - \frac{\tau}{T_\mathrm{s}}\sigma_k - \frac{\tau}{T_\mathrm{s}}\sigma_k \\ & + \frac{\tau}{T_\mathrm{s}} \underbrace{G\left(T_\mathrm{s}\left(\dot{x}_{k-1}^r - f_{k-1}\right) - T_\mathrm{s} B u_{k-1}\right)}_{\sigma_k - \sigma_{k-1} + O(T_\mathrm{s}^2)} \\ & + \frac{\tau}{T_\mathrm{s}}\sigma_{k-1} + O(\tau^2). \end{aligned} \quad (31)$$

Further simplifications lead to

$$\sigma(kT_\mathrm{s} + \tau) = \sigma_k - \frac{\tau}{T_\mathrm{s}}\sigma_k + \frac{\tau}{T_\mathrm{s}} G\left(T_\mathrm{s}\left(\Delta\dot{x}_k^r - \Delta f_k\right)\right) + O(\tau^2). \quad (32)$$

If $\dot{x}^r$ and f are smooth and bounded then

$$\sigma(kT_\mathrm{s} + \tau) = \sigma_k - \frac{\tau}{T_\mathrm{s}}\sigma_k + O(\tau^2). \quad (33)$$

Note that if $\sigma_k = O(T_\mathrm{s}^2)$, as was shown previously, then the maximum intersampling value of the sliding function is $O(T_\mathrm{s}^2)$. Hence

$$\sigma(kT_\mathrm{s} + \tau) = O\left(T_\mathrm{s}^2\right). \quad (34)$$

C. Lyapunov Stability of the Closed-Loop System

In this section, it will be shown that with discrete-time control defined by (18), it is possible to satisfy the Lyapunov condition (10) in discrete time.

Starting with the definition of the Lyapunov function in discrete-time, proportional to one defined by (6)

$$V_k = \sigma_k^2. \quad (35)$$

The difference of two consecutive values of the Lyapunov function in discrete time can be given by

$$V_{k+1} - V_k = \sigma_{k+1}^2 - \sigma_k^2 \quad (36)$$

where it is required that $V_{k+1} - V_k < 0$ for $\sigma_k \neq 0$ 0. However, it will be shown that $V_{k+1} - V_k < 0$ for $|\sigma_k| > O(T_\mathrm{s}^2)$. The condition $V_{k+1} - V_k < 0$ means that

$$\sigma_{k+1}^2 - \sigma_k^2 < 0. \quad (37)$$

If (27) is substituted into (37)

$$V_{k+1} - V_k = O\left(T_\mathrm{s}^4\right) - \sigma_k^2. \quad (38)$$

Note that if $|\sigma_k| > O(T_\mathrm{s}^2)$ then $V_{k+1} - V_k < 0$. Thus, (38) shows that σ_k is always converging toward a boundary of $O(T_\mathrm{s}^2)$ around the desired sliding-manifold and (34) shows that once σ_k reaches $O(T_\mathrm{s}^2)$ boundary it will tend to stay in that boundary.

IV. Disturbance Observer

A. Structure of the Observer

The structure of the observer is based on (1) under the assumption that all the plant parameter uncertainties, nonlinearities, and external disturbances can be represented as a lumped disturbance. As it is obvious, y is the displacement of the plant and is measurable. Likewise, $u(t)$ is the input to the plant and is also measurable. Hence, the nominal structure of the plant is defined as follows

$$\begin{aligned} m_{\mathrm{N}}\ddot{y} + c_{\mathrm{N}}\dot{y} + k_{\mathrm{N}}y &= T_{\mathrm{N}}u(t) - F_{\mathrm{d}} \\ F_{\mathrm{d}} &= T_{\mathrm{N}}h + \Delta T(\nu_{\mathrm{in}} + \nu_h) + \Delta m\ddot{y} \\ &\quad + \Delta c\dot{y} + \Delta k y \end{aligned} \tag{39}$$

where m_{N}, c_{N}, k_{N}, and T_{N} are the nominal plant parameters while Δm, Δc, Δk, and ΔT are the uncertainties of the plant parameters. Since y and $u(t)$ are measured, the proposed observer is of the following form

$$m_{\mathrm{N}}\ddot{\hat{y}} + c_{\mathrm{N}}\dot{\hat{y}} + k_{\mathrm{N}}\hat{y} = T_{\mathrm{N}}u - T_{\mathrm{N}}u_c \tag{40}$$

where $\hat{y}$ is the estimated position u is the plant control input and u_c is the observer control input. If $\hat{y}$ can be forced to track y, then the control input to the observer becomes $T_{\mathrm{N}}u_c = F_{\mathrm{d}}$, what can be easily verified by determining the value of the equivalent control for system (39), (40) in manifold (41). From the structure of it follows that control input to the observer u_c consists of the terms related to hysteresis effects $(T_{\mathrm{N}}h + \Delta T\nu_h)$, the terms related to the PZT parameters uncertainties $(\Delta m\ddot{y} + \Delta c\dot{y} + \Delta k y)$ and the term related to the uncertainty in the conversion parameter $(\Delta T\nu_{\mathrm{in}})$ thus estimating total disturbance [as defined in (39)] but not the components of the disturbance separately. The observer controller that is used is in the sliding-mode-control (SMC) framework. Selecting the following sliding manifold

$$\sigma_{\mathrm{obs}} = \lambda_{\mathrm{obs}}(y - \hat{y}) + (\dot{y} - \dot{\hat{y}}) \tag{41}$$

where λ_{obs} is a positive constant. If σ_{obs} is forced to zero then $\hat{y}$ is forced to track y. It is known from the analysis in the previous section that condition of the same form as (10) $\dot{\sigma}_{\mathrm{obs}} + D_{\mathrm{obs}}\sigma_{\mathrm{obs}} = 0$ guarantees $\sigma_{\mathrm{obs}} \to 0$. If (41) is plugged into $\dot{\sigma}_{\mathrm{obs}} + D_{\mathrm{obs}}\sigma_{\mathrm{obs}} = 0$ then

$$(\ddot{y} - \ddot{\hat{y}}) + (\lambda_{\mathrm{obs}} + D_{\mathrm{obs}})(\dot{y} - \dot{\hat{y}}) + \lambda_{\mathrm{obs}}D_{\mathrm{obs}}(y - \hat{y}) = 0 \tag{42}$$

where D_{obs} is a positive constant and it can be seen that the transients of the closed-loop system are defined by the roots $-\lambda_{\mathrm{obs}}$ and $-D_{\mathrm{obs}}$. The controller that will be used in the observer is the same as the controller defined by (18). From structure (40), it can be seen that the input matrix B in (18) is

$$B = \begin{bmatrix} 0 & -\dfrac{T_{\mathrm{N}}}{m_{\mathrm{N}}} \end{bmatrix}^{\mathrm{T}} \tag{43}$$

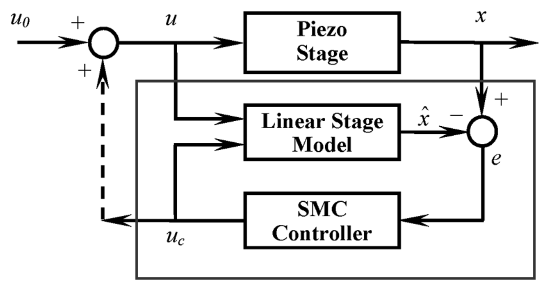

Fig. 2. Observer implementation.

and the matrix G in (18) for this case is

$$G = [\lambda_{\mathrm{obs}} \quad 1]. \tag{44}$$

Thus, after some simplifications, the controller can be

$$u_{c_k} = u_{c_{k-1}} - \frac{m_{\mathrm{N}}}{T_{\mathrm{N}}}\left(D_{\mathrm{obs}}\sigma_{\mathrm{obs}_k} + \frac{\sigma_{\mathrm{obs}_k} - \sigma_{\mathrm{obs}_{k-1}}}{T_{\mathrm{s}}}\right) \tag{45}$$

here

$$\sigma_{\mathrm{obs}_k} = \lambda_{\mathrm{obs}}(y_k - \hat{y}_k) + (y_k - y_{k-1})/T_{\mathrm{s}} - (\hat{y}_k - \hat{y}_{k-1})/T_{\mathrm{s}}.$$

The observer implementation is best described by Fig. 2. Positive feedback of u_c would, ideally, force the system to behave close to an ideal system defined by

$$m_{\mathrm{N}}\ddot{y} + c_{\mathrm{N}}\dot{y} + k_{\mathrm{N}}y = T_{\mathrm{N}}u_0(t) \tag{46}$$

where $u_0(t)$ is the uncompensated control input to the system. However, this is just the ideal case and in reality the dynamics of the observer would lead to differences between the real disturbance and the estimated disturbance.

B. Observer Dynamics

As it was mentioned previously, the dynamics of the observer has to be analyzed in order to see how close it is possible to force the system to behave ideally as defined by (46). Consider the state-space description of (39) and assuming that the disturbance F_{d} is matched

$$\dot{x} = Ax + Bu - Bd \tag{47}$$

where $F_{\mathrm{d}} = Bd$, and the matrices A and B are given by

$$A = \begin{bmatrix} 0 & 1 \\ -k_{\mathrm{N}}/m_{\mathrm{N}} & -c_{\mathrm{N}}/m_{\mathrm{N}} \end{bmatrix} \quad \text{and} \quad B = \begin{bmatrix} 0 \\ T_{\mathrm{N}}/m_{\mathrm{N}} \end{bmatrix}. \tag{48}$$

The discrete-time counterpart of (48) is

$$x_{k+1} = \Phi x_k + \Gamma u_k - \Gamma d_k \tag{49}$$

where the matrices Φ and Γ are given by

$$\Phi = \mathrm{e}^{AT_{\mathrm{s}}} \quad \text{and} \quad \Gamma = \int_0^{T_{\mathrm{s}}} e^{A\tau}Bd\tau. \tag{50}$$

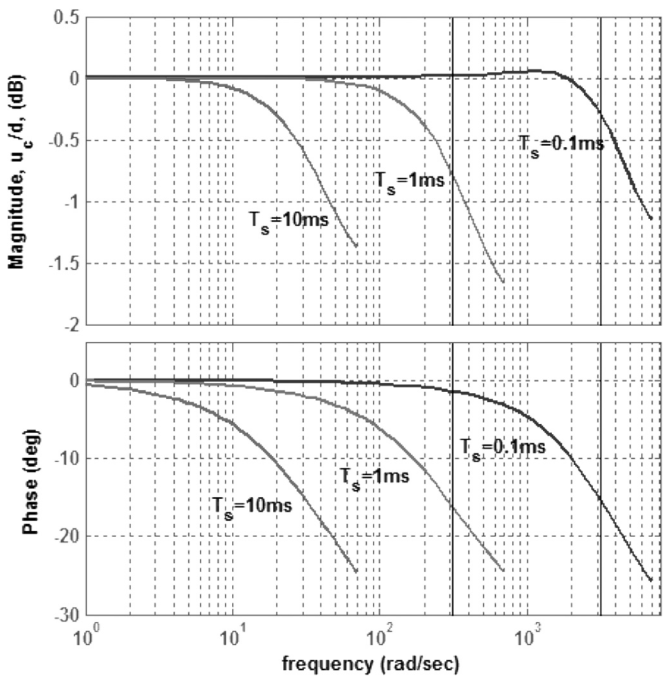

Fig. 3. Frequency response of estimated disturbance w.r.t. disturbance.

The disturbance observer is also of the form

$$\hat{x}_{k+1} = \Phi \hat{x}_k + \Gamma u_k - \Gamma u_{c_k}. \quad (51)$$

If (51) is subtracted from (49) then

$$e_{k+1} = x_{k+1} - \hat{x}_{k+1} = \Phi e_k - \Gamma \left(d_k - u_{c_k} \right). \quad (52)$$

The discrete-time transfer function of e_k can be found from

$$e_k = -(I \cdot z - \Phi)^{-1} \Gamma \left(u_{d_k} - u_{c_k} \right). \quad (53)$$

Similarly, the controller defined by (18) can be written in transfer function form

$$(1 - z^{-1}) u_{c_k} = -(GBT_\mathrm{s})^{-1} \left((1 + DT_\mathrm{s}) - z^{-1} \right) \sigma_{\mathrm{obs}_k}. \quad (54)$$

If $D = 1/T_\mathrm{s}$ and (54) is simplified further

$$u_{c_k} = -\frac{(GBT_\mathrm{s})^{-1}(2z - 1)}{z - 1} \sigma_{\mathrm{obs}_k}. \quad (55)$$

Note that $\sigma_{\mathrm{obs}_k} = G e_k$; therefore, using (53) and (55)

$$u_{c_k} = \frac{(GBT_\mathrm{s})^{-1}(2z-1) G (I \cdot z - \Phi)^{-1} \Gamma}{(z-1) + (GBT_\mathrm{s})^{-1}(2z-1) G (I \cdot z - \Phi)^{-1} \Gamma} d_k \quad (56)$$

From (56), it is possible to analyze the sensitivity of the disturbance observer w.r.t. disturbance. Fig. 3 shows the frequency response of the observer estimated disturbance w.r.t. disturbance for cases when the sampling-time is 10, 1, and 0.1 ms. For the observer characteristics shown in Fig. 3, the controller parameters are as follows: $D_\mathrm{obs} = \lambda_\mathrm{obs} = 1/T_\mathrm{s}$.

It will be interesting to see the effect inclusion of disturbance compensation has on the overall closed-loop system.

C. Closed-Loop Performance With the Disturbance Observer

In this section, the sensitivity of the controlled position with respect to disturbance will be analyzed. Consider (49), the open-loop transfer function can be written as

$$x_k = (I \cdot z - \Phi)^{-1} \Gamma (u_k - d_k). \quad (57)$$

For simplicity, (57) will be written as

$$x_k = H_\mathrm{OL}(z)(u_k - d_k). \quad (58)$$

Similar analysis can be done for the controller defined by (18), which can be written as

$$u_k = (GBT_\mathrm{s})^{-1} \frac{(1 + DT_\mathrm{s})z - 1}{z - 1} \sigma_k. \quad (59)$$

If $D = 1/T_\mathrm{s}$ and (59) is simplified further

$$u_k = (GBT_\mathrm{s})^{-1} \frac{2z - 1}{z - 1} G \left(x_k^r - x_k \right) = H_\mathrm{c}(z) \left(x_k^r - x_k \right). \quad (60)$$

If (60) is substituted into (58) and the estimated disturbance u_{c_k} is added to u_k

$$x_k = H_\mathrm{OL}(z) H_\mathrm{c}(z) \left(x_k^r - x_k \right) + H_\mathrm{OL}(z) \left(u_{c_k} - d_k \right). \quad (61)$$

If (56) is written as

$$u_{c_k} = H_\mathrm{Obs}(z) d_k \quad (62)$$

and substituted into (61) and after simplifications the following result is obtained

$$x_k = H_\mathrm{CL}(z) x_k^r + H_\mathrm{Dis}(z) d_k \quad (63)$$

where the transfer matrices $H_\mathrm{CL}(z)$ and $H_\mathrm{Dis}(z)$ are given by

$$H_\mathrm{CL}(z) = \left(I + H_\mathrm{OL}(z) H_\mathrm{c}(z) \right)^{-1} H_\mathrm{OL}(z) H_\mathrm{c}(z) \quad (64)$$

and

$$H_\mathrm{Dis}(z) = \left(I + H_\mathrm{OL}(z) H_\mathrm{c}(z) \right)^{-1} H_\mathrm{OL}(z) \left(H_\mathrm{Obs}(z) - 1 \right). \quad (65)$$

Note that the displacement is $y_k = C x_k$ where $C = [1\ 0]$

$$y_k = \mathrm{CH}_\mathrm{CL}(z) x_k^r + \mathrm{CH}_\mathrm{Dis}(z) d_k. \quad (66)$$

Now, it is possible to see the sensitivity of the controlled position w.r.t. the disturbance for the case of disturbance compensation. Note that if there was no disturbance compensation, then the transfer matrix $H_\mathrm{Dis}(z)$ would be

$$H_\mathrm{Dis}(z) = \left(I + H_\mathrm{OL}(z) H_\mathrm{c}(z) \right)^{-1} H_\mathrm{OL}(z). \quad (67)$$

Also, note that in the case of open-loop control the transfer matrix $H_\mathrm{Dis}(z)$ can be found from (58) after including the estimated disturbance u_c defined by (62) with the control input u. This would result with following form of $H_\mathrm{Dis}(z)$

$$H_\mathrm{Dis}(z) = H_\mathrm{OL}(z) \left(H_\mathrm{Obs}(z) - 1 \right) \quad (68)$$

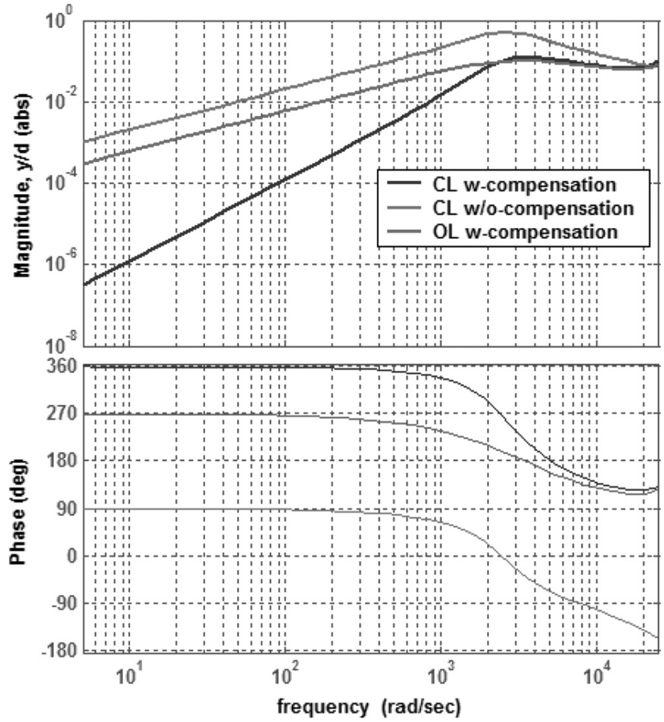

Fig. 4. Sensitivity (micrometer/volt) of the controlled position w.r.t. disturbance.

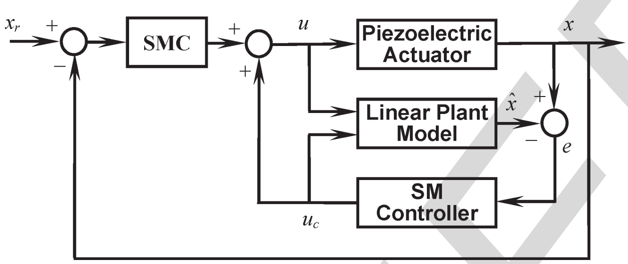

Fig. 5. Control scheme.

In Fig. 4 the sensitivity of the closed-loop system for the cases with and without disturbance compensation are shown along with open-loop system with disturbance compensation. Note that when disturbance compensation is included, the sensitivity of the controlled position with respected to disturbance is less than for the case without disturbance compensation (Fig. 5). This shows the effectiveness of combining the disturbance feed-forward term and the SMC controller. In the used design, the structure of the disturbance observer is such that the same controller is used in the main control loop and in the disturbance observer loop thus simplifying the overall design procedure.

V. Experiments

In order to illustrate the effectiveness of the proposed control simulation and experiments are carried out on a single axis of a three-axis piezostage manufactured by Physik Instrumente supplied by E-664 power amplifier. Table I shows the specifications of the piezostage. The controller hardware used is the DSPACE DS1103 with the control algorithm executed on MATLAB and SIMULINK with real-time link to DS1103.

TABLE I
Properties of the Piezostage

Symbol	Quantity	Value in SI
m_N	nominal mass	1.5×10^{-3} kg
c_N	nominal damping	220 N·s/m
k_N	nominal stiffness	300000 N/m
f_r	resonant frequency	350 Hz
T_N	em transformation ratio	0.3 N/V

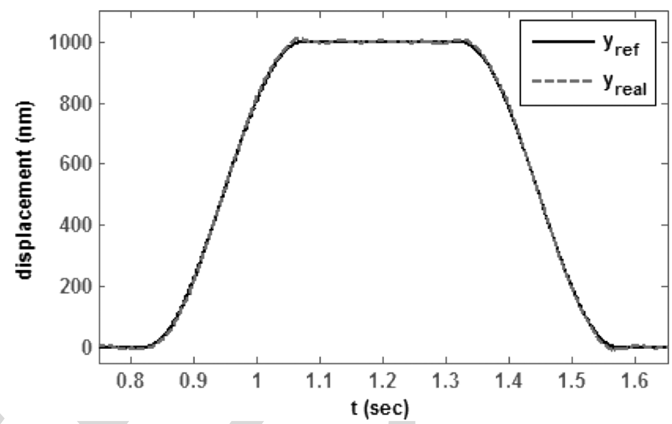

Fig. 6. Open-loop with compensation response to a trapezoidal reference.

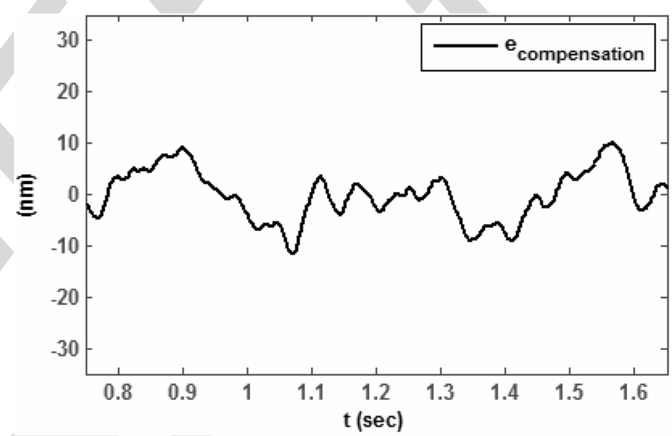

Fig. 7. Compensation error for open-loop with compensation case.

Initial experiments were conducted on the system with just open-loop disturbance compensation. Figs. 6 and 7 show the response and compensation error with open-loop control. This can easily be understood from the results of the sensitivity analysis shown in Fig. 4. As it can be seen that, although there is no closed-loop controller, the open-loop control with disturbance compensation produces good results as was expected.

Further experiments are conducted with the system with closed-loop SMC with disturbance compensation. Fig. 8 and 9 show the response to a position reference similar to that used in the open-loop case. The results show that the proposed controller produces good results.

As a means of comparison, the system is experimented with PID controller. The results are shown in Fig. 10 and 11. As it can be seen, the traditional controller such PID fails to provide very good results.

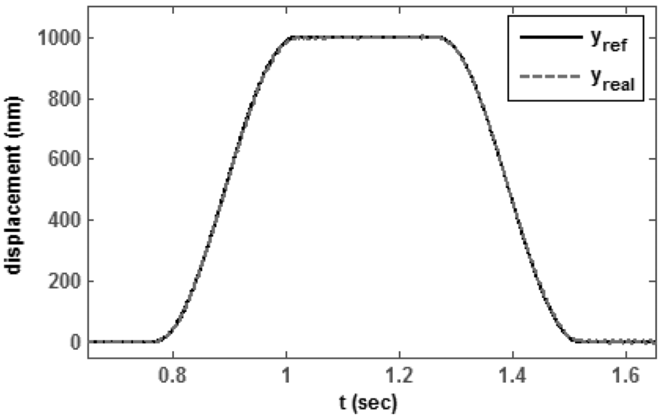

Fig. 8. Response with SMC and compensation.

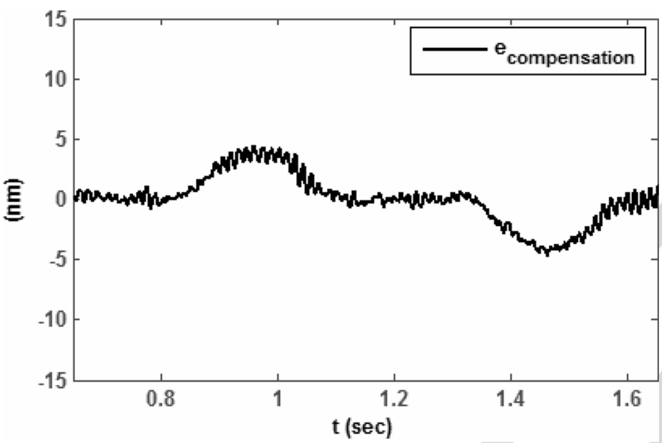

Fig. 9. Tracking performance of SMC with compensation.

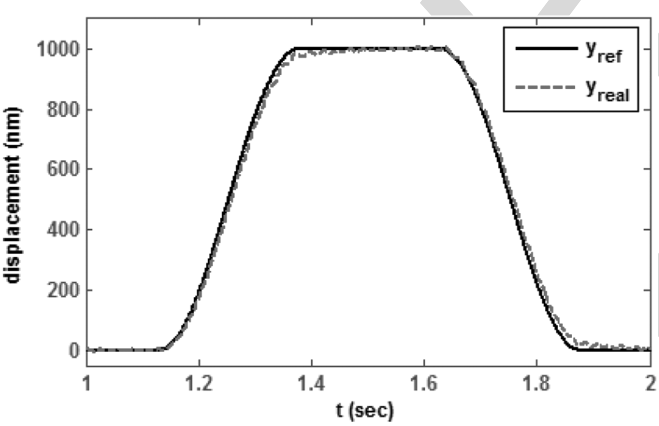

Fig. 10. Closed-loop PID control.

VI. Conclusion

In this paper, the design of a discrete-time sliding mode controller based on the Lyapunov is presented. The controller is analyzed for a general system and shown to have very good performance. It was shown that, similar to [14], the zero-order hold causes a limitation on the sliding-mode accuracy. However, it was shown that with partial knowledge of system dynamics, it is possible to drive the system within $O(T_s^2)$ of the desired sliding manifold S.

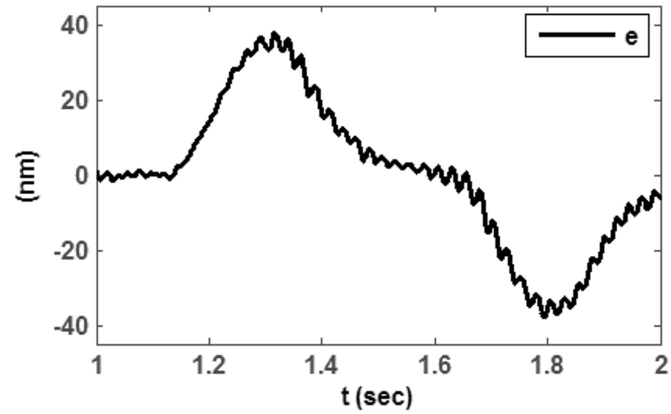

Fig. 11. Tracking performance of PID control.

It was also shown that the introduction of disturbance compensation along with discrete-time SMC in the control of a piezostage improves the tracking performance. This can be very useful for applications where simplicity of the controller as well as high-precision control is required.

References

[1] B. Zhang and Z. Zhu, "Developing a linear piezomotor with nanometer resolution and high stiffness," *IEEE/ASME Trans. Mechatronics*, vol. 2, no. 1, pp. 22–29, Mar. 1997.

[2] M. Goldfarb and N. Celanovic, "Modeling piezoelectric stack actuators for control of micromanipulation," *IEEE Control Syst. Mag.*, vol. 17, no. 3, pp. 69–79, Jun. 1997.

[3] R. Banning, W. L. de Koning, and J. M. T. A. Adriaens, "Modeling piezoelectric actuators," *IEEE/ASME Trans. Mechatronics*, vol. 5, no. 4, pp. 331–341, Dec. 2000.

[4] K. K. Leang and S. Devasia, "Iterative feedforward compensation of hysteresis in piezo poisitioners," in *Proc. 42nd IEEE Conf. Decision and Control*, Maui, HI, 2003, pp. 2626–2631.

[5] P. Krejci and K. Kuhnen, "Inverse control of systems with hysteresis and creep," *Proc. Inst. Electr. Eng.—Control Theory Appl.*, vol. 148, no. 3, pp. 185–192, May 2001.

[6] R. Banning, W. L. de Koning, J. M. T. A. Adriaens, and K. R. Koops, "State-space analysis and identification for a class of hysteretic systems," *Automatica*, vol. 37, no. 12, pp. 1883–1892, 2001.

[7] B. M. Chen, T. H. Lee, C.-C. Hang, Y. Guo, and S. Weerasooriya, "An $H\infty$ almost disturbance decoupling robust controller design for a piezoelectric bimorph actuator with hysteresis," *IEEE Trans. Control Syst. Technol.*, vol. 7, no. 2, pp. 160–174, Mar. 1999.

[8] Y. I. Somov, "Modeling physical hysteresis and control of a fine piezo-drive," in *Proc. Int. Conf. Phys. and Control*, 2003, vol. 4, pp. 1189–1194.

[9] J. H. Xu, "Neural network control of piezo tool positioner," in *Proc. Can. Conf. Electr. and Comput. Eng.*, 1993, vol. 1, pp. 333–336.

[10] K. K. Tan, T. H. Lee, and H. X. Zhou, "Micro-positioning of linear-piezoelectric motors based on a learning nonlinear PID controller," *IEEE/ASME Trans. Mechatronics*, vol. 6, no. 4, pp. 428–436, Dec. 2001.

[11] S. B. Chang, S. H. Wu, and Y. C. Hu, "Submicrometer overshoot control of rapid and precise positioning," *J. Amer. Soc. Precis. Eng.*, vol. 20, no. 3, pp. 161–170, May 1997.

[12] V. I. Utkin, "Sliding mode control in discrete-time and difference systems," in *Variable Structure and Lyapunov Control*, A. S. I. Zinober, Ed. London, U.K.: Springer-Verlag, 1994, pp. 87–107.

[13] K. D. Young, V. I. Utkin, and U. Ozguner, "A control engineer's guide to sliding mode control," *IEEE Trans. Control Syst. Technol.*, vol. 7, no. 3, pp. 328–342, May 1999.

[14] W.-C. Su, S. V. Drakunov, and U. Ozguner, "An O(T2) boundary layer in sliding mode for sampled-data systems," *IEEE Trans. Autom. Control*, vol. 45, no. 3, pp. 482–485, Mar. 2000.

[15] K. Ohnishi, M. Shibata, and T. Murakami, "Motion control for advanced mechatronics," *IEEE/ASME Trans. Mechatronics*, vol. 1, no. 1, pp. 56–67, Mar. 1996.

[16] S. C. Chapra and R. P. Canale, *Numerical Methods for Engineers*, 3rd ed. Singapore: WCB/McGraw-Hill, 1998.

[17] K. Abidi and A. Šabanoviç, “A study of discrete-time sliding mode control robustness analysis and experimental verification,” in *Proc. 24th IASTED Conf. MIC*, Innsbruck, Austria, Feb. 16–18, 2005.

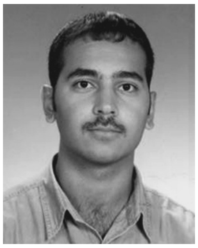

Khalid Abidi received the B.S. degree in mechanical engineering from Middle East Technical University, Ankara, Turkey, and the M.S. degree in electrical engineering and computer science from Sabanci University, Istanbul, Turkey, in 2002 and 2004, respectively. He is currently working toward the Ph.D. degree in electrical and computer engineering at National University of Singapore, Kent Ridge, Singapore.

He is currently with National University of Singapore, Kent Ridge, Singapore, as a Research Assistant. His research interests include analysis of dynamic systems, adaptive control, iterative learning control, robust control, high-precision motion control, and microsystems.

Asif Šabanovic (M’92–SM’04) received the B.S. degree in electrical engineering, in 1970, and the M.S. and Dr. Eng. degrees, all from University of Sarajevo, Sarajevo, Bosnia-Herzegovina.

He is a Full Professor with Sabanci University, Istanbul. Since 1970 until 1991, he has been with Energoinvest-Institute for Control and Computer Sciences, Sarajevo, Bosnia-Herzegovina. Since 1991, he has been with University of Sarajevo, Department of Electrical Engineering, Sarajevo, Bosnia-Herzegovina. In 1975–1976, he was a Visiting Researcher with Institute of Control Science—Moscow. Visiting Professor with California Institute of Technology—CALTECH, Pasadena, in 1984–1985, Hitachi Chair Professor with Keio University, Yokohama, in 1991–1992, Full Professor with Yamaguchi University, Ube, in 1992–1993, Visiting Professor with University of Maribor—Maribor, Slovenia (Acad. Year 1986, 1988, 1989), Head of CAD/CAM and Robotics Department with Tubitak—Marmara Research Centre, Istanbul, in 1993–1995, and Head of Engineering Department of B.H. Engineering and Consulting, in 1995–1999. His fields of interest include control systems, motion control systems, robotics, mechatronics, and power electronics.

AUTHOR QUERIES

AUTHOR PLEASE ANSWER ALL QUERIES

AQ1 = Please provide the expanded form of the acronym “r.h.s.”
AQ2 = Figure 5 was uncited in the body. It was inserted here. Please check if appropriate.
AQ3 = Please provide page range in Ref. [17].
AQ4 = Please provide the expanded form of the acronym “CAD/CAM.”
AQ5 = Please provide the expanded form of the acronym “B.H.”
Note: Refs. [12], [13], and [15] were not cited anywhere in the text.

END OF ALL QUERIES